Journal of Magnetism and Magnetic Materials 412 (2016) 181–184

Contents lists available at ScienceDirect

Journal of Magnetism and Magnetic Materials

journal homepage: www.elsevier.com/locate/jmmm

AlOx barrier growth in magnetic tunnel junctions for sensor applications

S. Knudde [a,b,*], G. Farinha [a,b], D.C. Leitao [a,b], R. Ferreira [c], S. Cardoso [a,b], P.P. Freitas [a,c]

[a] INESC-MN, Microsystems and Nanotechnologies, Rua Alves Redol 9, 1000-029 Lisboa, Portugal
[b] Instituo Superior Tecnico, Universidade de Lisboa, 1000-029 Lisboa, Portugal
[c] INL International Iberian Nanotechnology Laboratory, Braga, Portugal

ARTICLE INFO

Article history:
Received 10 February 2016
Received in revised form
21 March 2016
Accepted 2 April 2016
Available online 6 April 2016

Keywords:
Magnetic tunnel junctions
Amorphous barriers
Magnetic sensors
AlOx

ABSTRACT

Magnetic tunnel junction (MTJ) research has been focused on MgO-based crystalline structures due to high tunnel magnetoresistance (TMR), despite requiring a more severe process control than previous generations of MTJ stacks based on amorphous barriers (e.g. AlOx). In this work, we study the electrical transport properties in AlOx barriers in MTJ sensors fabricated using Ion beam sputtering and remote plasma oxidation. Amorphous barriers were prepared from oxidation of thin Al films, deposited in single step barrier (SSB-Al 1 nm/oxidation) or double step barrier (DSB-Al 0.5 nm/oxidation/Al 0.5 nm/oxidation) structures. We show tunable resistance-area products (RxA) ranging from ≈10 Ω μm^2 (suited for nano devices) up to ≈100 kΩ μm^2 (suited for large area sensors) with TMR above 30%. For all geometries studied, the structures have a coercivity free linear response and require none or one annealing step. This makes them very competitive for all industrial applications where the TMR level is not the dominant specification to meet.

1. Introduction

Magnetic tunnel junctions (MTJs) sensing devices are key nowadays for accurate detection of magnetic fields [1,2]. MTJs are already widely used in magnetic read heads due to the high tunneling magnetoresistance (TMR) at room temperature. Moreover, TMR sensors enable roadmap solutions for several applications, such as magnetometers, biochips, surface mapping, rotation monitoring, servomotors feedbacks [3–5]. The tunnel barrier of MTJ sensors are either made of specific crystalline materials enabling coherent tunneling, (MgO, MgAlOx) [6] or amorphous materials (AlOx, TiOx, etc.) [7,8]. While MgO has a higher TMR signal compared to AlOx, the latter remains competitive in terms of fabrication easiness and noise levels [9]. For example, MgO barriers can reach several hundreds of % in TMR but the process to achieve this requires very careful deposition and proper crystallization of the barriers and CoFeB electrodes upon annealing. MgO based junctions are thus delicate and expensive to produce, especially in sensing devices where a soft free layer is desired and NiFe is a commonly used material. However, NiFe has a fcc crystalline structure while the high TMR ratio comes from a bcc-phase lattice matched interface between CoFeB and MgO [10]. In this case the crystallinity of NiFe will hinder proper crystallization of CoFeB upon annealing and the TMR will be reduced [11] . Strategies are then required to overcome the propagation of the NiFe fcc crystallinity into the CoFeB, e.g. by use of a Ta dusting layer between the NiFe and CoFeB [12]. In contrast, amorphous barrier junctions can easily incorporate NiFe in the free layer without significant changes in the tunneling properties. In addition, the characteristics of both the insulating layer interfaces, such as surface roughness, contamination, defects and crystallinity, play a key role in the spin-tunneling effect [11]. Also here, amorphous materials offer higher control and reproducibility than crystalline materials, e.g. AlOx is less sensitive to contamination than MgO.

AlOx can be produced by oxidizing the Al in room atmosphere, whereas MgO requires a stringent deposition control in systems with very low base pressure to eliminate water contamination. Therefore, in applications where tunnel junctions reaching 40–50% TMR can be used, AlOx MTJs become more desirable as they can be easily produced with wider processing window. AlOx barriers can be produced by sputtering metallic Al and then oxidizing the metal film to form the oxide barrier. The oxidation of Al to AlOx will increase its volume by roughly 30% [13]. This increase in volume will heal defects in the ultra thin layer of AlOx. Some methods have been demonstrated to be reliable for oxidation of a thin Al film: (i) oxygen molecule from the atmosphere will have a very weak oxidation, with low penetration, requiring several

* Corresponding author at: INESC-MN, Microsystems and Nanotechnologies, Rua Alves Redol 9, 1000-029 Lisboa, Portugal.
E-mail address: sknudde@inesc-mn.pt (S. Knudde).

http://dx.doi.org/10.1016/j.jmmm.2016.04.008
0304-8853/

minutes to one hour of oxidation of <1 nm thick Al layer. The integration of such a process in an automated sequence for large scale production is also an obstacle; (ii) using an oxygen plasma will effectively oxidize barriers up to ≈1 nm thickness in less than a minute, while allowing a good control of the oxidation depth; (iii) an oxygen ion beam will have a very effective oxidation, ideal for ≈2 nm thick barriers leading to RxA products in the MΩ μm^2.

In this work, we use remote plasma for the oxidation of Al films thinner than 1 nm, to create amorphous barriers in magnetic tunnel junction stacks leading to RxA values of less than 10 kΩ μm^2. To reach values of RxA in the 10–100 kΩ μm^2 range, two iterations of deposition and oxidation steps were performed. We then compare single (SSB) and double step barriers (DSB) of equal nominal thicknesses in their current–voltage (*I–V*) characteristic and conclude that for barrier thicknesses (t_{Al}) > 0.8 nm, DSB sensors have superior properties due to more efficient oxidation of the Al layer leading to higher TMR and more symmetric $TMR(V_{bias})$.

2. Experimental details

MTJ thin film stacks were deposited from metallic targets in a Nordiko 3000 ion beam sputtering tool [14]. The deposition conditions for Al were optimized to have continuous films down to 0.5 nm, which was achieved at a deposition rate of 0.016 nm/s. The Al thin films were then oxidized by remote plasma using the assist gun (Fig. 1d) [15]. The plasma was composed of a mixture of

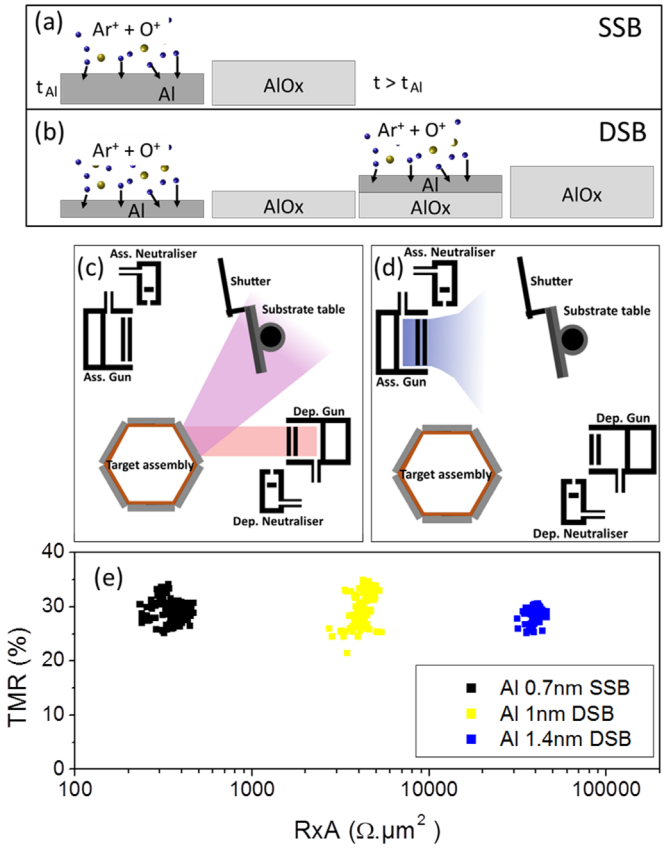

Fig. 1. Illustration of the oxidation process for (a) SSB and (b) DSB samples, with a remote plasma energy of 20 eV. Schematics of the deposition tool during: (c) deposition step, highlighting the ion beamhitting the target from which the atoms are sputtered and then deposited on the substrate; and (d) oxidation step, highlighting the remote plasma created in the assist gun. (e) TMR versus RxA for selected representative samples with different RxA (Buffer/IrMn 18/CoFe 3/Ru 0.6/CoFeB 4/AlOx d/CoFeB 3/Ru 15; thicknesses in nm). The lower range of RxA is easily achieved with SSB, but higher RxA requires DSB.

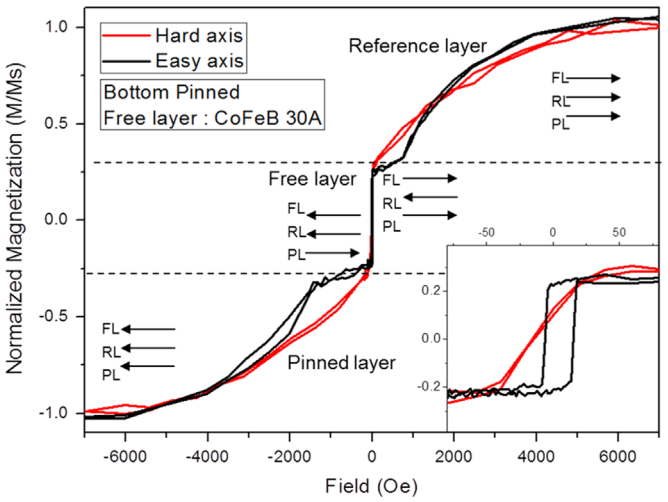

Fig. 2. Easy and hard axes M(H) of unpatterned bottom pinned MTJ (Buffer/IrMn 18/CoFe 3/Ru 0.6/CoFeB 4/AlOx d/CoFeB 3/Ru 15 nm). Three regions can be distinguished: at low field the free layer reversal, at higher fields the pinned layer reversal in the negative field values and the reference layer in positive values. Inset shows a detail of the free layer behavior along both axes.

20 sccm Oxygen and 4 sccm Argon as described elsewhere [14,15], working pressure during oxidation was 6×10^{-4} Torr and the plasma energy 20 eV. Barriers were either produced by deposition of a single layer of Al of the desired barrier thickness followed by oxidation (SSB). Or by deposition of a layer of Al, half the desired barrier thickness and then oxidation, followed by a second layer of Al and another oxidation step (DSB), e.g.: SSB=Al 1 nm/ Oxidation, DSB=Al 0.5 nm/Oxidation/Al 0.5 nm/ Oxidation. All Al thicknesses referred in this work are the nominal thicknesses (t_{Al}).

All MTJ stacks have a synthetic antiferromagnetic (SAF) reference layer pinned on IrMn. The samples were annealed 30 min at 250 °C followed by a slow cooldown under a 1 T field to set exchange bias at the CoFe/IrMn interface. The exchange bias field obtained reaches 75 mT. In addition, the presence of a SAF provides a stable reference layer above 100 mT, while the operating range of the sensors are typically inferior to 20 mT (Fig. 2). The thin film stacks were characterized by Vibrating Sample Magnetometer (VSM) and current in plane tunneling (CIPT). The samples were patterned using optical lithography and ion milling etching in rectangular shapes and sizes from 1 μm × 20 μm to 3 μm × 50 μm. Patterned devices were mapped for TMR, RxA and *I–V* curves.

3. Results and discussion

3.1. Unpatterned MTJs

Fig. 3a shows TMR as a function of oxidation time for different t_{Al}. These results were obtained for both SSB and DSB using CIPT in unpatterned samples. The TMR increases with oxidation time up to a maximum value which depends on t_{Al}. This behavior is consistent with the presence of non-magnetic metallic remains (non-oxidized Al) in the barrier. A maximum TMR_{max} = 40%, is e.g. achieved with 15 s of oxidation in a SSB sample with t_{Al} = 0.7 nm. This value then decreases due to overoxidation. At this point the oxidation can damage the bottom electrode [16]. Overall, the maximum of TMR decreases with increasing t_{Al}, indicating that the oxidation process becomes inefficient for thick layers, in agreement with previously observed data [17]. For the deposition rate and oxidation parameters studied, while SSB Samples with t_{Al} < 0.8 nm achieved 40% TMR, although above such thickness